A. AZMI
S.A. SATA
F.S. ROHMAN
N. AZIZ

School of Chemical Engineering, Engineering Campus, Universiti Sains Malaysia, Seri Ampangan 14300 Nibong Tebal, Seberang Perai Selatan, Penang, Malaysia

DYNAMIC OPTIMIZATION OF LOW-DENSITY POLYETHYLENE PRODUCTION IN TUBULAR REACTOR UNDER THERMAL SAFETY CONSTRAINT

Article Highlights
- The dynamic optimization of low density polyethylene (LDPE) industry is carried out
- Mass and energy balances of LDPE are validated using industrial data
- The expression of reactor temperature under critical condition is developed for thermal safety
- The safety component can be inserted in problem optimization as an inequality path constraint
- The maximization of monomer under thermal safety is solved using orthogonal collocation method

Abstract
A commercial low-density polyethylene (LDPE) which is produced by the polymerization process of ethylene in the presence of initiators in a long tubular reactor is the most widely used in polymer industry. The highly exothermic nature of the LDPE polymerization process and the heating-cooling prerequisite in the tubular reactor can lead to various problems, particularly safety in terms of thermal runaway and productivity, i.e., decreasing monomer conversion. Therefore, model-based optimization of an industrial LDPE tubular reactor under thermal safety consideration is required to be implemented. A first principle model for this process is developed and validated using industrial data. Mass and energy balances have been derived from kinetics of LDPE polymerization. Thereafter, an expression of reactor temperature under critical condition is developed and incorporated in the reference model for the thermal safety study. In order to ensure the process is thermally safe and meets the desired product grade, the constrained dynamic optimization is proposed to maximize the conversion of the monomer using orthogonal collocation (OC). The dynamic optimization result shows that the maximum reaction temperature under critical condition constraint can be satisfied by optimizing the reactor jacket. Moreover, it is achieved without jeopardizing the monomer conversion and the product grade.

Keywords: low-density polyethylene, tubular reactor, dynamic optimization, thermal safety.

Low density polyethylene (LDPE) is a major polymer that is vastly used as feedstock in the production of packaging, adhesives, coatings, and films.

The robustness quality of LDPE's properties leads to various usages of such a polymer which is considered as an exclusive and high demand commodity [1,2]. The production and consumption rates of LDPE are reported to be 20.31 million tons in 2015 [3]. Market study reveals that the projection of LDPE consumption and production rates would continue to increase steadily, which justifies its continuous improvement for the past 40 years [4,5].

LDPE is produced by the polymerization process of ethylene in the presence of initiators either in

a long tubular reactor, as shown in Figure 1, or in a well-stirred autoclave reactor. On an industrial scale, most LDPEs are produced in tubular reactors [6]. The advantages of using LDPE tubular technology over autoclave reactors include better heat removal and cheaper organic peroxides that can be used as initiators. Moreover, there is no need to use α-olefins which can cause the formation of side branches in the polymer chain that is generated by the radical polymerization process itself [7].

The monomer conversion (X_M) in the tubular reactor is reported to be very low, which is in the range of 20-30% per pass [8]. Considering the requirement for high compression power and the expensive cost of raw materials, the utility cost of LDPE production in the tubular reactor is quite high. The X_M, which is proportional to profits has always been the focus for researchers and engineers in this field. However, there are several issues that complicate the improvement task.

Ethylene, along with initiators and chain transfer agents (CTA), are used to produce LDPE *via* free radical polymerization in extreme conditions, typically at pressures of 1,500-3,000 atm and temperatures of 50-350 °C [9]. Ethylene polymerization is a highly exothermic reaction and a rapid process. Once the polymerization process occurs, the reaction temperature would rise rapidly until all the injected initiator is exhausted [10]. A sharp increase in temperature and of conversion will occur in a short reaction zone signalling to the development of the ethylene polymerisation process. This process occurs rapidly and can lead to a thermal runaway if the temperature rise is not controlled. Under normal operating conditions, the use of maximum temperature limit (T_{max}) alone is probably adequate to ensure the free radical polymerization process runs safely, however, for a reactor behaving in an abnormal condition, the use of the T_{max}

value will be an inappropriate indicator of a safety process [11]. Thus, maximum temperature under a critical condition (Tc_{max}) constraint must be imposed as a constraint to ensure the process is thermally safe.

Heat exchange failure or cooling system breakdown at any spot in this reactor may lead to a runaway condition and fatal failure. Therefore, it is essential to conduct a study to determine the optimal condition of operating parameters that can guarantee safe operation in the critical condition. However, this kind of study presents various challenges, particularly when it can lead to a reduction in production output. Monomer conversion, which is proportional to profit calculation, will most probably be reduced to facilitate the optimal condition of this study.

Numerous optimization studies that consider maximum X_M have been reported by previous researchers [8,12]. However, none of the studies consider thermal safety constraints. To bridge the gap, the dynamic optimization with thermal safety constraint must be carried out. The main objective of this work is to carry out dynamic optimization using two optimization problems. The first problem is to maximize the X_M under maximum temperature (T_{max}) constraint whereas the second problem is to maximize the X_M under maximum critical temperature (Tc_{max}). For both optimization problems, the reactor jacket (T_J) is considered as a control variable. Since the dynamic optimization method applied required a reliable model of the process, in this work, a mathematical model of LDPE polymerization in a tubular reactor that is validated with industrial data is developed.

Process modeling of LDPE tubular reactor

The first principle model which provides the kinetic and fundamental theory [13], is selected to describe the process in detail. The first principle model of the LDPE tubular reactor incorporates the conser-
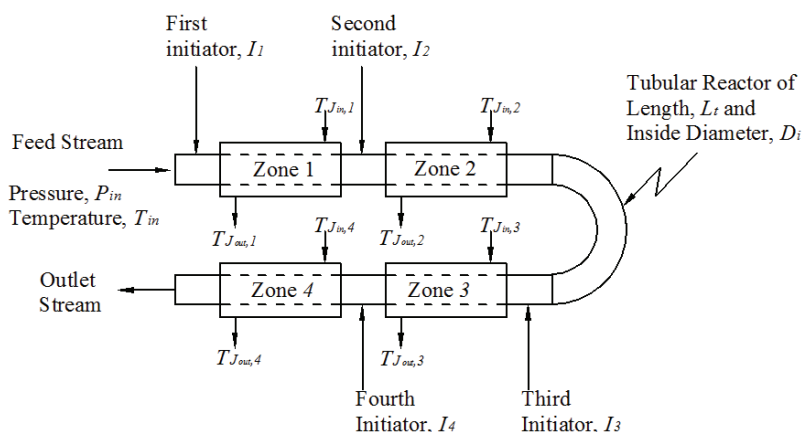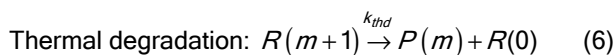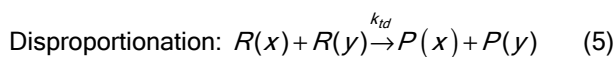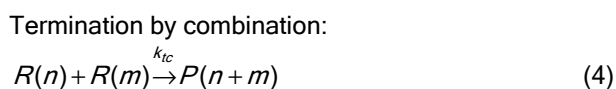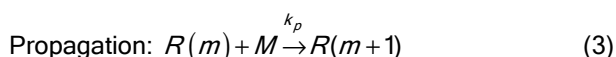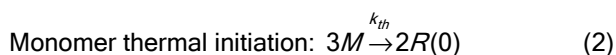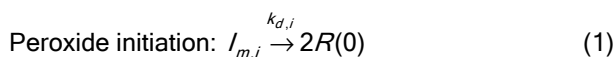

Figure 1. Schematic diagram of an industrial LDPE tubular reactor.

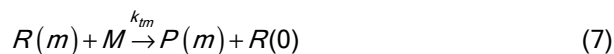vation of mass, energy, and momentum balance in the reactor.

Reaction mechanism and kinetic model

LDPE is produced through a free radical polymerization of ethylene at high pressure and temperature. The main reactions involved in LDPE polymerization are chain initiation by initiator decomposition, followed by propagation and termination. Additional reaction mechanisms involved are chain transfer to monomer, chain transfer to polymer, chain transfer to solvent, and backbiting. The main reactions which are peroxide initiation, monomer thermal initiation, chain propagation, termination by combination, termination by disproportionation and thermal degradation are all common to free radical polymerization [14]. The main reactions of free radical polymerization are summarized in Eqs. (1)-(6) [6]:

Peroxide initiation: $I_{m,i} \xrightarrow{k_{d,i}} 2R(0)$ (1)

Monomer thermal initiation: $3M \xrightarrow{k_{th}} 2R(0)$ (2)

Propagation: $R(m) + M \xrightarrow{k_p} R(m+1)$ (3)

Termination by combination:

$R(n) + R(m) \xrightarrow{k_{tc}} P(n+m)$ (4)

Disproportionation: $R(x) + R(y) \xrightarrow{k_{td}} P(x) + P(y)$ (5)

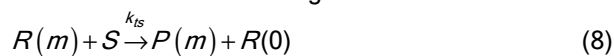Thermal degradation: $R(m+1) \xrightarrow{k_{thd}} P(m) + R(0)$ (6)

In addition to the main reactions which occur in all free radical polymerization processes, several side reactions are also present. The inter-molecular chain transfer, produces long chain branches (LCB) in LDPE. The back-biting or intramolecular chain transfer reaction is the major source of short chain branches (SCB) in LDPE. Both SCB and LCB are important characteristics of LDPE [8]. The content of SCB in a typical LDPE is 30 per 1000 CH_2, whereas the content of LCB is 10-30 per molecule. Meanwhile, the formation of vinyl (V_i) and vinylidene (V_{id}) unsaturated groups are closely associated with the scission of secondary and tertiary radicals [8]. The reaction schemes for the side reactions are summarized in Eqs. (7)-(12) [7]. A detailed explanation on the polymerization reaction mechanisms and molecular structure of each component involved in Eqs. (1)-(12) can be found in Agrawal's [8] work:
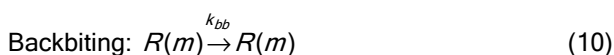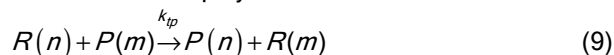
Chain transfer to monomer:

$R(m) + M \xrightarrow{k_{tm}} P(m) + R(0)$ (7)

Chain transfer to transfer agent:

$R(m) + S \xrightarrow{k_{ts}} P(m) + R(0)$ (8)

Chain transfer to polymer:

$R(n) + P(m) \xrightarrow{k_{tp}} P(n) + R(m)$ (9)

Backbiting: $R(m) \xrightarrow{k_{bb}} R(m)$ (10)

β-Scission of secondary radical:

$R(m) \xrightarrow{k_{\beta}} P(m) + R(0)$ (11)

$\beta 1$-Scission of tertiary radical:

$R(m) \xrightarrow{k_{\beta 1}} P(m) + R(0)$ (12)

Reactor model equations

The first principle model is expressed as the mass balances of initiator, solvent, monomer, free radicals, and dead polymer in conjunction with the energy balances at the reaction and jacket sides along the reactor. The reactor scheme for this study is shown in Figure 1. The model takes into account four initiator injection points, variable density, viscosity, and velocity of the reaction stream. The derivative of axial velocity with respect to axial length in materials balance is ignored in the present study as it is considered negligible [15,16]. The developed model uses data from reported industrial production. The mass balances with regards to each respective component in the LDPE tubular reactor polymerization process are given by Eqs. (13)-(18) [7]:

Peroxide initiator mass balance:

$$v \frac{dC_{I_i}}{dz} + 2f_{d,x}K_{d_i}C_{I_i} = 0$$ (13)

Monomer mass balance:

$$v \frac{dC_M}{dz} + K_p C_M \lambda_0 + 2K_{th}C_M^3 + K_{tm}C_M \lambda_0 = 0$$ (14)

Solvent mass balance:

$$v \frac{dC_S}{dz} + K_{ts}C_S \lambda_0 = 0$$ (15)

Methyl group/1000 CH_2 mass balance:

$$v \frac{dC_{Me}}{dz} + K_{bb}\lambda_0 = 0$$ (16)

Vinyl group/1000 CH_2 mass balance:

$$v\frac{dC_{Vi}}{dz} + K_{\beta1}\lambda_0 = 0 \tag{17}$$

Vinylidene group/1000 CH_2 mass balance:

$$v\frac{dC_{Vid}}{dz} + K_{\beta}\lambda_0 = 0 \tag{18}$$

The energy balance for the reaction and cooling zones are represented by Eqs. (19) and (20), respectively [7]:

$$\frac{dT}{dz} = \frac{1}{\rho C_P v}\left[-\Delta H K_p C_M \lambda_0 - \frac{4U(T-T_J)}{D_i}\right] \tag{19}$$

$$\frac{dT}{dz} = \frac{1}{\rho C_P v}\left[-\frac{4U(T-T_J)}{D_i}\right] \tag{20}$$

Meanwhile, the pressure profile in the reaction mixture is expressed in Eq. (21):

$$\frac{dP}{dz} = -\frac{2f_r v^2}{D_{in}} \tag{21}$$

The expressions for the moments of live radical (λ_i) distribution are defined by Eqs. (22)-(24) [7,15]:

$$v\frac{d\lambda_0}{dz} = 2fK_{d_i}C_{I_i} + 2K_{th}C_M^3 - (K_{tc}+K_{td})\lambda_0^2 \tag{22}$$

$$v\frac{d\lambda_1}{dz} = 2fK_{d_i}C_{I_i} + 2K_{th}C_M^3 - (K_{tc}+K_{td})\lambda_0\lambda_1 - \\ -(K_{tm}C_M + K_{ts}C_S + K_{thd} + K_{bb} + K_{\beta} + K_{\beta1})\times \\ \times(\lambda_1-\lambda_0) + K_p C_M \lambda_0 + K_{tp}(\lambda_0\mu_2 - \lambda_1\mu_1) \tag{23}$$

$$v\frac{d\lambda_2}{dz} = 2fK_{d_i}C_{I_i} + 2K_{th}C_M^3 - (K_{tc}+K_{td})\lambda_0\lambda_2 - \\ -(K_{tm}C_M + K_{ts}C_S + K_{thd} + K_{bb} + K_{\beta} + K_{\beta1})\times \\ \times(\lambda_2-\lambda_0) + K_p C_M \lambda_0 + 2K_p C_M \lambda_1 + K_{trp}(\lambda_0\mu_3 - \lambda_2\mu_1) \tag{24}$$

The concentration of the radical moments is considered to be pseudo-stationary as inferred from previous studies [7,15], therefore Eqs. (22)-(24) are converted into Eqs (25)-(27):

$$\lambda_0 = \sqrt{\frac{2fK_{d_i}C_{I_i} + 2K_{th}C_M^3}{(K_{tc}+K_{td})}} \tag{25}$$

$$\lambda_1 = \frac{2fK_{d_i}C_{I_i} + 2K_{th}C_M^3 + K_p C_M \lambda_0 + K_{tp}\lambda_0\mu_2 + (K_{tm}C_M + K_{ts}C_S + K_{thd} + K_{bb} + K_{\beta} + K_{\beta1})\lambda_0}{(K_{tc}+K_{td})\lambda_0 - (K_{tm}C_M + K_{ts}C_S + K_{thd} + K_{bb} + K_{\beta} + K_{\beta1}) + K_{tp}\mu_1} \tag{26}$$

$$\lambda_2 = \frac{2fK_{d_i}C_{I_i} + 2K_{th}C_M^3 + K_p C_M \lambda_0 + 2K_p C_M \lambda_1 + K_{tp}\lambda_0\mu_3 + (K_{tm}C_M + K_{ts}C_S + K_{thd} + K_{bb} + K_{\beta} + K_{\beta1})\lambda_0}{(K_{tc}+K_{td})\lambda_0 - (K_{tm}C_M + K_{ts}C_S + K_{thd} + K_{bb} + K_{\beta} + K_{\beta1}) + K_{tp}\mu_1} \tag{27}$$

The expression of live radical moments, as shown in Eqs. (25)-(27) is also implemented as a solution to molecular weight distribution [15,16].

The mass balance on a polymer model based on the reaction mechanism is given in the Eqs. (28)-(30):

$$v\frac{d\mu_0}{dz} = K_{td}\lambda_0^2 + \frac{1}{2}K_{tc}\lambda_0^2 + \\ +(K_{tm}C_M + K_{ts}C_S + K_{thd} + K_{bb} + K_{\beta} + K_{\beta1})\lambda_0 \tag{28}$$

$$v\frac{d\mu_1}{dz} = K_{td}\lambda_0\lambda_1 + K_{tc}\lambda_0\lambda_1 + \\ +(K_{tm}C_M + K_{ts}C_S + K_{thd} + K_{bb} + K_{\beta} + K_{\beta1})\lambda_1 + \\ +K_{tp}(\lambda_1\mu_1 - \lambda_0\mu_2) \tag{29}$$

$$v\frac{d\mu_2}{dz} = K_{td}\lambda_0\lambda_2 + K_{tc}(\lambda_0\lambda_2 + \lambda_1^2) + \\ +(K_{tm}C_M + K_{ts}C_S + K_{thd} + K_{bb} + K_{\beta} + K_{\beta1})\lambda_2 + \\ +K_{tp}(\lambda_2\mu_1 - \lambda_0\mu_3) \tag{30}$$

The closure method of the polymer moment (μ_3) is represented by Eq. (31) [17]:

$$\mu_3 = \frac{\mu_2}{\mu_0\mu_1}\left(2\mu_0\mu_2 - \mu_1^2\right) \tag{31}$$

The equations of live radical moments which are shown in Eqs. (25)-(27) and the differential equations of polymer moments which are shown in Eqs. (28)-(30) are crucial in mass balance as they enable the determination of polymer properties which includes molecular weight (*MW*) and melt flow index (*MFI*). The kinetic parameter K_x values are estimated via the parameter estimation study. The values of K_x are not exposed due to proprietary reasons. The simulated data is then validated by using data from an industrial company which operates in Malaysia.

Properties of the mixture

The density and the specific heat capacity of the reaction mixture considered in this study are denoted as the composition of pure ethylene. The equations

are in the function of pressure and temperature as prescribed by Buchelli *et al.* [18]. The density and the specific heat capacity of the reaction mixture are approximated by Eqs. (32) and (33), respectively:

$$\rho_m = \left((X_e / \rho_e) + ((1 - X_e) / \rho_{pe}) \right)^{-1} \tag{32}$$

$$Cp_m = X_e Cp_e + (1 - X_e) Cp_{pe} \tag{33}$$

Heat properties

The overall heat transfer coefficient (U) is calculated directly from the temperature differences and heat transferred in the reactor using Eq. (34) [19]:

$$U = \left((Q / A) \Delta T_{lm} \right) \tag{34}$$

The value of heat transfer (Q) is calculated from the heat rise of the water coolant stream as in Eq. (35):

$$Q = \left(\dot{m}_J Cp_J \left(T_{J,out} - T_{J,in} \right) \right) \tag{35}$$

and the log mean temperature (ΔT_{lm}) is given as in Eq. (36):

$$\Delta T_{lm} = \frac{\left((T_{P,in} - T_{J,out}) - (T_{P,out} - T_{J,in}) \right)}{\ln \left((T_{P,in} - T_{J,out}) / (T_{P,out} - T_{J,in}) \right)} \tag{36}$$

Production output

Eqs. (37)-(39) represent the calculations for monomer conversion (X_M), weight-average molecular weight (MW) [8] and melt flow index (MFI) [20]:

$$X_M = 100 \left[1 - \left(\frac{C_M}{C_{M_0}} \right) \right] \tag{37}$$

$$MW = 28.05 \left(\frac{\mu_2 + \lambda_2}{\mu_1 + \lambda_1} \right) \tag{38}$$

$$MFI (\text{g/10min}) = (2.75e33)(gMW \times 10^{-4})^{-7.61} \tag{39}$$

Assessment criteria for the severity of a runaway condition

The assessment criteria for the severity of a runaway condition is based on ΔT_{ad} value. This value is chosen since it shows the amount of reactor temperature rise for LDPE polymerization in the tubular reactor. A severity criterion of potential for runaway condition which is listed in Table 1, is assessed according to the Zurich Insurance Company and is commonly used in the chemical industry [11]. If the assessment occurs on a three-level scale, the upper levels for "critical" and "catastrophic" may be considered one level, "high".

Table 1. Assessment criteria for the severity of a runaway condition [11]

Simplified	Extended	ΔT_{ad} / °C	Order of magnitude of Q, kJ kg^{-1}
High	Catastrophic	>400	>800
	Critical	200-400	400-800
Medium	Medium	50-100	100-400
Low	Negligible	<50 and no pressure	<100

Based on the literature [4,12,21] the temperature rise due to introduction of the initiator under normal operating conditions is observed to be in the range of 100-200 °C. The temperature rise has a higher possibility to increase even higher from this range, especially in the event of a heat exchange failure. According to the Zurich hazard analysis (ZHA), an adiabatic rise of temperature of more than 200 °C can be classified as high severity for a runaway reaction and requires safety technical measures [11]. For this reason, the present study considers a temperature increase of 200 °C and above to be critical. The rise in temperature can be considered as the reaction temperature under critical condition.

Reaction temperature under critical condition (T_c) and maximum temperature under critical condition (T_{cmax})

When the heat transfer failure occurs, the energy balance in Eq. (19) zones become Eq. (40):

$$\frac{dT_c}{dz} = \frac{1}{\rho C_P v} \left[-\Delta H K_p C_M \lambda_0 \right] \tag{40}$$

Thus, the profile of T_c represents the reaction temperature under critical conditions while T in Eq. (19) represents the reaction temperature running under normal conditions. Both T and T_c have different profiles with different maximum temperatures. In the reaction temperature running under normal conditions (T), its maximum value is directly taken from the plant operating manual, while in the case of the reaction temperature under critical conditions (T_c), its maximum value is decided by the sum of T_{in} and ΔT_{ad}.

The critical condition scenario is designed at the reaction zone only since this is the area where the highly exothermic polymerization reaction occurs. Therefore, failure or breakdown is most likely to occur in this zone rather than in the cooling zone [11].

Dynamic optimization study

The dynamic optimization technique applied which is based on the direct-discretization method is orthogonal collocation (OC). The OC method is executed by using the dynopt code package within

Matlab R2015a that has been developed by Cizniar [22] which utilizes an algorithm developed by Cuthrell and Biegler [23]. In this approach, state and control variables are parameterized simultaneously by using OC on finite elements. The iteration step for differential equation solver and the optimizer are computed simultaneously [24].

In this study, the orthogonal collocation (OC) on finite elements is used to convert the original optimization problems into nonlinear programming (NLP) problems [25,26]. The resulting NLP problems are solved by sequential quadratic programming (SQP). The gradients of the objective function, states and the constraints required in the SQP are differentiated by using Matlab symbolic function. The basic procedure followed is: 1) discretize both inputs and states using a Lagrange polynomial; 2) discretize the state equation with their initial conditions for selected interval time, *i.e.*, the differential equations are satisfied only at a finite number of interval length (*via* orthogonal collocation). These two steps modify the discretized optimization problem into a standard nonlinear program; 3) specify an initial guess for the decision variables, number of collocation and interval length; 4) calculate for the optimal solution of the specified objective function and generate the optimal trajectories by using the SQP method. The basic algorithm of OC can be described in Figure 2.
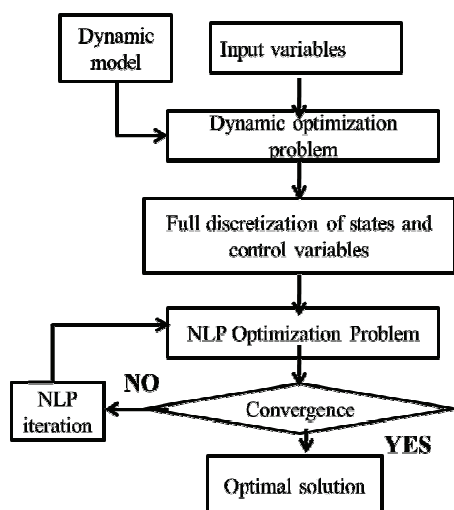

Figure 2. Basic procedure of orthogonal collocation method.

The Optimization Toolbox with *fmincon* (find minimum of constrained nonlinear multivariable function) command was used to solve SQP problems within the MATLAB® environment. In the search iteration, the convergence criterions which must be predetermined are TolX and TolFun. TolX is a minimum allowable size of a step. If the SQP acquires a

searching step that is smaller than TolX, the iterations finalized. TolFun is a minimum allowable on the change in the value of the objective function during a searching step. For those algorithms, if $|F(x_n) - F(x_{n+1})|$ < TolFun, the iterations end. TolX and TolFun can be specified as 10^{-6}, in order to obtain an accurate solution.

Problem optimization formulation

Two problem optimization formulations are considered in this study. The first problem is to maximize the X_M under maximum temperature (T_{max}) constraint whereas the second problem is to maximize the X_M under maximum critical temperature (Tc_{max}). The only different between Problem 1 and Problem 2 is the path constraint imposed on each optimization formulation. In Problem 1, the reactor is considered to behave normally, whereas in the reactor in Problem 2 is assumed to run under critical condition. The terminal inequality constraint applied for both problems is *MFI*. The reactor jacket (T_J) is considered as a control variable. The dynamic optimization formulations for the two problems which consist of the objective function, decision variables, process, bounds and constraints are shown as follows:

Problem 1 - Maximum conversion with maximum reactor temperature (T_{max}).

The problem can be described as:

Given	The fixed final length and the allowable range of LDPE's *MFI*
Optimize	The reactor jacket temperature profile
Searching parameter	Monomer, solvent, initiators feed flow rate and reactor inlet pressure
So as to maximize	The conversion of the monomer
Subject to constraints	Model equation, bounds on the feed flow rate, bounds on the reactor jacket temperature
Subject to path constraints	Maximum reactor temperature (T_{max})

Mathematically the optimization problem can be written as in Eq. (41):

$$\text{Problem 1:} \quad \max_{T_{J,i}(z), F_{M0}, F_{S0}, F_{I,i0}, P_{in}} X_M \qquad (41)$$

Subject to:

$$M\dot{x}(z) = f(x(z), u(z), p, z) \qquad \text{(Eqs. (13)-(31))}$$

$$0.69 \le \frac{T_{J,i}}{T_{J,i(ref)}} \le 1.69 \qquad \text{(Lower and upper control variable bound)}$$

$$0.96 \le \frac{F_{M0}}{F_{M0\,(ref)}} \le 1.02 \;;$$ (Lower and upper parameter bound)

$$0.95 \le \frac{F_{S0}}{F_{S0\,(ref)}} \le 1.22$$

$$0.23 \le \frac{F_{I,i0}}{F_{I,i0\,(ref)}} \le 1.27 \;;$$

$$0.93 \le \frac{P_{in}}{P_{in\,(ref)}} \le 1.03$$

$$0.93 \le \frac{MFI}{MFI_{ref}} 1.03$$ (Lower and upper MFI bound)

$$\frac{z_f}{z_{f\,ref}} = 1.00$$ (Terminal equality constraint)

$$T_{max} / T_{max\,ref} \le 1.03$$ (Inequality path constraint)

Problem 2 - Maximum conversion with maximum critical reactor temperature (Tc_{max}).

The problem can be described as:

Given	The fixed final length and the allowable range of LDPE's MFI
Optimize	The reactor jacket temperature profile
Searching parameter	Monomer, solvent, initiators feed flow rate and reactor inlet pressure
So as to maximize	The conversion of the monomer
Subject to constraints	Model equation, bounds on the feed flow rate, bounds on the reactor jacket temperature
Subject to path constraints	Maximum critical reactor temperature (Tc_{max})

Mathematically the optimization problem can be written as in Eq. (42):

$$\text{Problem 2:} \quad \max_{T_{J,i}(z),F_{M0},F_{S0},F_{I,i0},P_{in}} X_M \qquad (42)$$

Subject to:

$$M\dot{x}(z) = f(x(z), u(z), p, z)$$ (Eqs. (13)-(31))

$$0.69 \le \frac{T_J}{T_{J\,(ref)}} \le 1.69$$ (Lower and upper control variable bound)

$$0.96 \le \frac{F_{M0}}{F_{M0\,(ref)}} \le 1.02 \;;$$ (Lower and upper parameter bound)

$$0.95 \le \frac{F_{S0}}{F_{S0\,(ref)}} \le 1.22$$

$$0.23 \le \frac{F_{I,i0}}{F_{I,i0\,(ref)}} \le 1.27 \;;$$

$$0.93 \le \frac{P_{in}}{P_{in\,(ref)}} \le 1.03$$

$$0.93 \le \frac{MFI}{MFI_{ref}} 1.03$$ (Lower and upper MFI bound)

$$\frac{z_f}{z_{f\,ref}} = 1.00$$ (Terminal equality constraint)

$$T_{c\,max} / T_{max\,ref} \le 1.24$$ (Inequality path constraint)

The bounds for the variable and parameters in Problem 1 and Problem 2 have been chosen based on the industrial data.

RESULTS AND DISCUSSION

The results of the modeling and optimization are presented and discussed in this section. In order to quantify the accuracy of the model, the comparison between the developed model and industrial data is carried out [27]. Then, the R-squared (R^2) obtained is used to assess the model accuracy and validity. The validated model is then used for the safety study. In the safety study, the T_c profile obtained is analyzed. In the optimization part, the results of the control variable trajectory, optimum parameter values, reactor temperature, and monomer conversion are analyzed with respect to thermal safety constraint consideration. For clarification, only relative values are displayed due to confidentiality reasons.

Model validation

Figures 3 and 4 show the model predictions for the temperature and the monomer conversion profiles versus the industrial data. The end product melt flow index (MFI) property obtained from the developed model also shows a satisfactory prediction with small error, 0.39%. It is observed that the model can predict the profiles very well with R-squared (R^2) values of 0.991 and 0.989 obtained for the reactor temperature and the monomer conversion (X_M) profiles are very close to 1.

The temperature profile in Figure 3 shows there are eight zones, which consist of four reactions and four cooling zones that exist in the LDPE tubular reactor. In the reaction zones, a sharp temperature peak is observed due to the highly exothermic rise of the polymerization reaction which generates a free radicals reaction between the feed in the initiator and the monomer. Monomer conversion (X_M) also indicates a fast escalation, and according to this temperature peak almost all of the initiator is consumed at this point. Due to no reaction occuring, X_M stays constant until another initiator is injected in the next react-
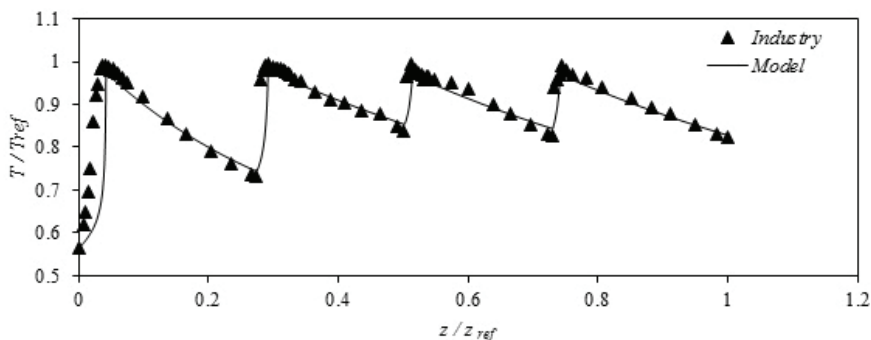
Figure 3. Reactor temperature, T profile of industrial case and model prediction.
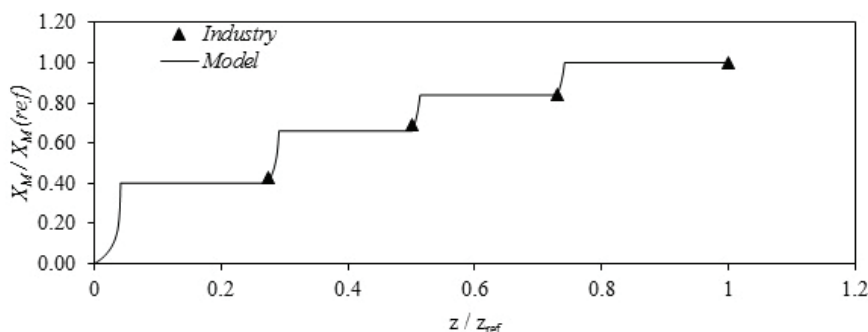

Figure 4. Monomer conversion, X_M profile of industrial case and model prediction.

ion zone. In the second zone, the reaction mixture is cooled down to the optimal temperature level for the half-life decomposition of the second initiator. Initiator disassociation is highly dependent on temperature and will be inefficient if the temperature exceeds its half-life temperature [16]. This inefficiency will reduce the initiation reaction and propagation rate thus reducing the monomer conversion value.

In the cooling zone, the temperature of the reaction mixture is cooled down steadily using a counter-current heat exchanger. This steady cooling process is to decrease the formation rate of a polymer-rich layer on the inner wall of the tubular reactor. The second initiator is injected in the third zone to aggravate the monomer conversion, as shown in Figure 4. This initiator is also exhausted soon after its injection into the reactor. The reaction mixture is again cooled in the fourth zone to the suitable level for the half-life of the third initiator, which generates the high efficiency of the initiator. These processes are repeated in the subsequent zone until the eighth zone where the product will undergo further separation and treatment processes.

Reaction temperature under critical condition (T_c) for reference model

The reaction temperature profiles in normal and critical operating conditions are shown in Figure 5.
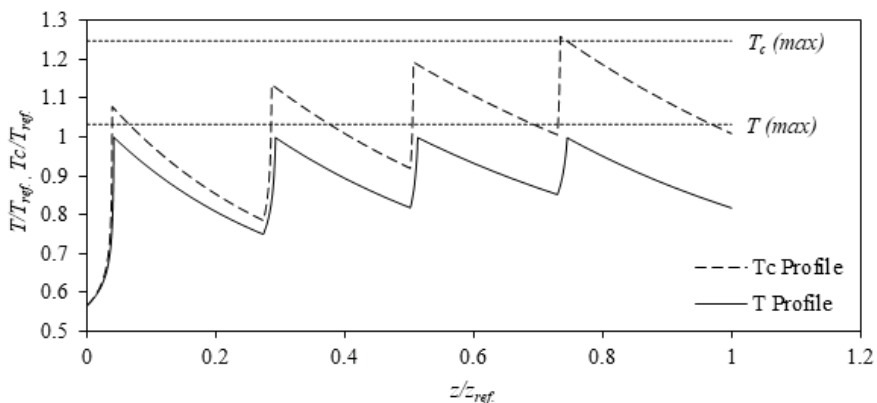

Figure 5. Reactor temperature (T) and critical reactor temperature (T_c) profiles of Base Case (reference model) across the tubular reactor.

The maximum reaction temperature (T_{max}) is used as an upper bound for normal conditions whereas the maximum critical reaction temperature (Tc_{max}) is used as an upper bound for the process in the event a reactive system cannot exchange energy with its surroundings (critical condition).

Here, it is clearly seen that the reactor peak temperature under critical condition (T_c) significantly rises beyond the operational T_{max} limit of 1.03. Therefore, the use of the T_{max} is impractical since the reaction temperature already exceeded the limit. In order to ensure that the LDPE tubular reactor polymerization is thermally safe, a new value for maximum reaction temperature under critical condition ($T_{c,max}$) must be introduced. As shown in Table 1, a process can be classified as critical when the adiabatic temperature rise (ΔT_{ad}) is more than 200 °C, therefore $T_{c,max}$ value is determined by adding up ΔT_{ad} of 200 °C with reactor inlet temperature (T_{in}).

With regards to the reaction process running under critical conditions, it can be observed from Figure 5 that the reaction critical temperature profile (T_c) already exceeds $T_{c,max}$ thus indicating that the present industrial LDPE tubular reactor produces an adiabatic temperature rise ΔT_{ad} of more than 200 °C which is considered as high severity for a runaway condition according to the Zurich hazard analysis (ZHA) [18]. This approach is a pre-assessment method to predict how far the temperature will rise adiabatically during the critical condition.

From Figure 5, it can be observed that the T_c profile has a significant trend change from the original T profile, as shown in Figure 5. At $z/z_{ref.} = 0 - 0.042$, where the first reaction occurs, the T/T_{ref} peak is 0.995 while the T_c/T_{ref} peak rises to 1.079, as shown in Figure 5. The T_c peak rises even higher in the next three reaction zones, located at $z/z_{ref.} = 0.2738 - 0.2928$, $z/z_{ref.} = 0.5019 - 0.5133$ and $z/z_{ref.} = 0.7300 - 0.7452$. The highest T_c/T_{ref} peak observed is 1.2592 that is obtained at the fourth reaction zone ($z/z_{ref.} = 0.7300 - 0.7452$). This is largely due to the high inlet temperature for each of the reaction zones as a result

of heat exchange absence, thus causing the sharp increment in the T_c profile as shown in Figure 5. The obvious way to ensure the T_c profile satisfies the $T_{c,max}$ is by reducing the peak T profile in Figure 5, however, it will reduce the X_M as well since the peak T profile and X_M are proportionally related. Consequently, the dynamic optimization study has to be carried out so that the X_M can be either increased or maintained while ensuring the T_c profile satisfies the $T_{c,max}$.

Optimization

These studies aim to maximize the monomer conversion for the LDPE tubular reactor running under maximum reaction temperature (T_{max}) and critical temperature constraints ($T_{c,max}$). For Problem 1, T_{max} constraints with bounds on the decision variables are imposed in the optimization problem, while in Problem 2, $T_{c,max}$ constraints with bounds on the decision variables are imposed.

The optimum results consist of the objective function (X_M), T_{max}, $T_{c,max}$ and *MFI* values of both Problems 1 and 2 are tabulated in Table 2. The melt flow index (*MFI*) is the parameter which is commonly practiced in the global LDPE manufacturing industry. It acts as an indicator of the molecular weight (*Mw*) and is favoured over other parameters because of its rapid and simple determination [20]. The results shown in Table 2 are the optimum reactor output achieved with optimal parameter values and trajectory of T_J as shown in Table 3 and Figure 6, respectively. The resulting optimization profiles of X_M, T, and T_c are shown in Figures 7-9, respectively. From Table 2, it can be observed that the $X_M/X_{M(ref)}$ in Problem 1 increases to 1.14. In Problem 1, temperature, T/T_{ref} peak is allowed to increase up to the maximum limit of 1.03 and this allows for extra monomer conversion to occur in the reaction zones.

From Table 2, it can be seen that the final $X_M/X_{M(ref)}$ obtained for Problem 2 is 1.10, which is higher than the Base Case. Compared to Problem 1, the final $X_M/X_{M(ref)}$ of Problem 2 is slightly lower than the former. In Problem 2, the maximum T/T_{ref} peak

Table 2. Results for maximize conversion of using different constraints

Problem	Constraint	$X_M/X_{M(ref)}$	$T_{max}/T_{max(ref)}$	$T_{c,max}/T_{max(ref)}$	$MFI/MFI_{(ref)}$
1	Max. reaction temperature, T_{max}	1.14	1.03	1.29	1.00
2	Max. critical temperature, $T_{c,max}$	1.10	1.03	1.25	1.00

Table 3. Optimal values of parameter variables (p_x) for maximize conversion with different constraints study

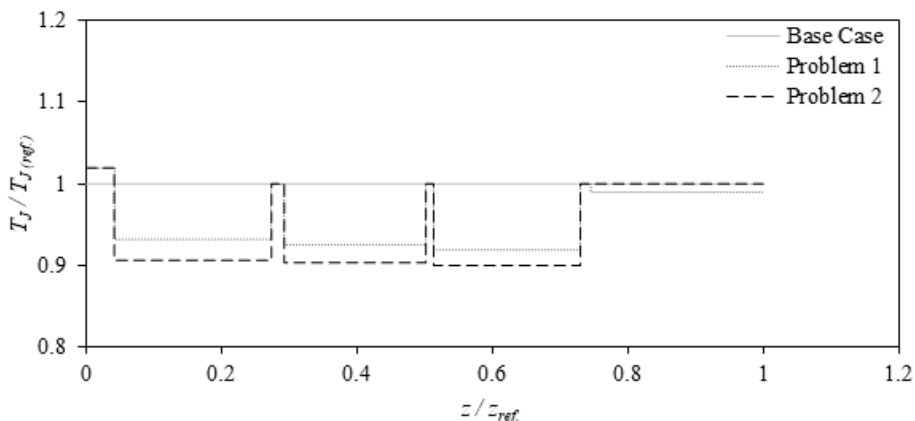| Problem	$F_{M0}/F_{M0(ref)}$	$F_{S0}/F_{S0(ref)}$	$F_{I,10}/F_{I,10(ref)}$	$F_{I,20}/F_{I,20(ref)}$	$F_{I,30}/F_{I,30(ref)}$	$F_{I,40}/F_{I,40(ref)}$	$P_{in}/P_{in(ref)}$
1	0.98	1.00	1.05	1.00	0.92	0.90	1.00
2	0.98	1.00	1.05	0.99	0.91	0.70	1.00

Figure 6. Reactor jacket temperature profiles across the tubular reactor.
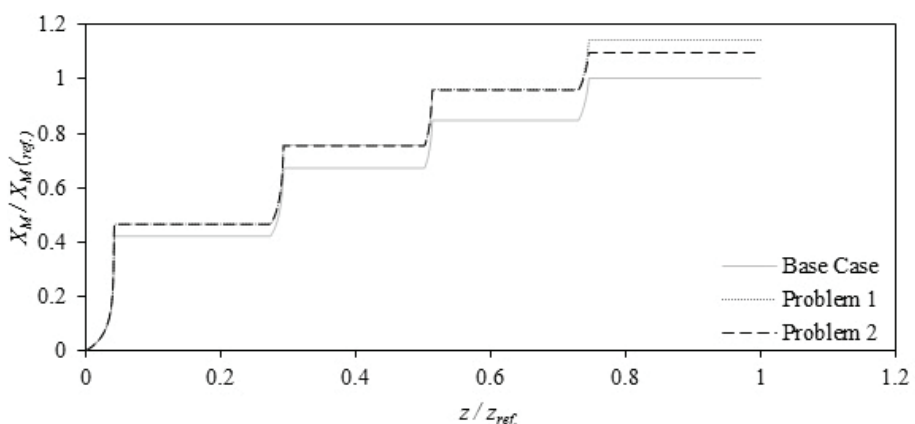

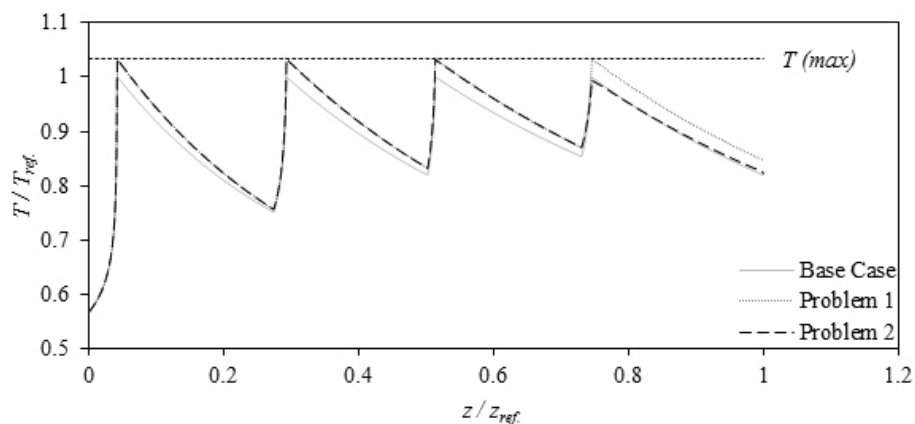*Figure 7. Monomer conversion profiles of Base Case, Problem 1 and Problem 2.*

Figure 8. Comparison of reactor temperature profiles of Base Case, Problem 1 and Problem 2.

obtained is 1.0260, which is lower than the maximum T/T_{ref} peak obtained in Problem 1. This is because, in Problem 2, the maximum reaction critical temperature constraint ($T_{c,max}$) is imposed, therefore the reduction in Problem 2 peak temperature occurs to ensure that the trajectory of the reaction critical temperature (T_c) satisfies the $T_{c,max}$ constraint. It is also observed in Table 2 that both problems satisfy the *MFI* grade

ranges. This is due to the presence of terminal inequality constraints at both problem optimization formulations. Maintaining polymer product within the specified grade is a primary performance indicator in LDPE production.

Figure 9 shows that the maximum peak temperature of T_c of Problem 1 is 1.29, which is obtained at the end of the fourth reaction zone 4R (at $z/z_{ref.}$ =
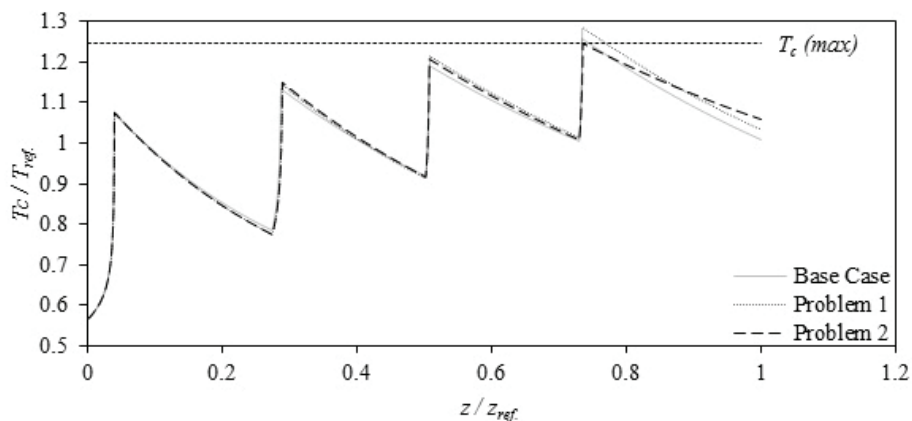
Figure 9. Comparison of reactor critical temperature profiles of Base Case, Problem 1 and Problem 2.

= 0.7452). This T_c/T_{ref} value exceeds $T_{c,max}$, indicating that the process does not compel thermal safety constraints. Therefore, adding reaction temperature constraint (T_{max}) alone would not be sufficient to ensure a thermal safety process. Figure 9 shows that the reaction temperature under critical condition T_c for Problem 2 successfully satisfies the maximum critical temperature ($T_{c,max}$) imposed on the optimization problem. However, it comes at the cost of a slightly lower conversion percentage. In a different optimization study carried out by Srinivasan, Palanki and Bonvin [28] using the batch reactor, they reported a similar reduction trend in conversion as a result of thermal safety constraint. This reduction is obtained in order to bring down the peak temperature. For the thermal safety constraint study, usually, the maximum peak temperature is lowered to facilitate the safety tolerance value [19]. For this reason, the monomer conversion is reduced as well since it is proportionally related to reaction temperature [29]. By tracking the optimal T_J trajectory obtained in Problem 2, the on-spec of LDPE grade can be produced within thermal safety precautions.

CONCLUSION

In the present paper, three main studies have been carried out to optimize LDPE production in a tubular reactor under thermal safety constraint which are process modelling, thermal safety risk assessment and optimization of tubular reactor process under thermal safety constraint. For the process modelling, it has been observed that the model can accurately predict the profiles of the reactor temperature and the monomer conversion with values of R^2 close to 1. The comparison of the product properties at the reactor end also showed a satisfactory agreement

where a low percentage of error was observed between the model and industrial data.

On the thermal safety risk assessment aspect, the present industrial LDPE tubular reactor has produced an adiabatic temperature rise (ΔT_{ad}) of more than 200 °C, which is considered as high severity for a runaway condition. For this reason, an optimal set of parameters need to be determined to ensure that ΔT_{ad} should not exceed 200 °C in the event of a cooling failure.

The dynamic optimization result has shown that an increase in monomer conversion has been achieved by both problem optimization formulations. The increment was obtained by optimal parameter values and trajectory of jacket temperature. Although Problem 1 has higher conversion than Problem 2, nevertheless the Problem 2 result has satisfied the thermal safety constraint $T_{c,max}$. These results demonstrate that $T_{c,max}$ constraint must be incorporated for a thermal safety operation since the T_{max} constraint is insufficient to protect the reactor, particularly in the event of cooling failure.

List of symbols

A_i Inside pipe area, cm^2

A_o Outside pipe area, cm^2

$A_{x,i}$ Frequency factor of x process with i-th number, l/(s cm^3/mol·s)

bb Backbiting, -

$C_{x,i}$ Concentration x component with i-th number, mol/cm^3

D_{in} Inside diameter of reactor, cm

D_e Equivalent diameter, cm

D_{Ji} Inner diameter of jacket wall, cm

$E_{x,i}$ Activation energy of x process with i-th number, cal/mol

e Ethylene, -

F_x Mass flow rate of x component, kg/h

f_x	Initiation efficiency of x-th peroxide, -
f_r	Fanning friction factor, -
G_c	Jacket volumetric flux rate, cm^3/s
ΔH_p	Heat of polymerization, cal/mol
h_i	Reactor side heat transfer coefficient, cal/(cm^2·K)
h_o	Outside film heat transfer coefficient, cal/(cm^2·K)
h_w	Heat transfer coefficient of reactor wall, cal/(cm^2·K)
$K_{d,i}$	Rate constant of peroxide initiation with i-th number, l/s
K_{th}	Rate constant of monomer thermal initiation, l/s
K_p	Rate constant of propagation, l/(mol·s)
K_{td}	Rate constant of termination by thermal degradation, l/(mol·s)
K_{thd}	Rate constant of termination by disproportionation, l/(mol·s)
K_{trm}	Rate constant of chain transfer to monomer, l/(mol·s)
K_{trp}	Rate constant of chain transfer to polymer, l/mol·s
K_{trs}	Rate constant of chain transfer to solvent, l/s
K_β	Rate constant of β-scission to secondary radical, l/s
$K_{\beta 1}$	Rate constant of β-scission to tertiary radical, l/s
K_m	Thermal conductivity of reaction mixture, cal/(cm·s·K)
K_w	Thermal conductivity of reactor wall, cal/(cm·s·K)
K_J	Thermal conductivity of jacket water, cal/(cm·s·K)
L	Length of reactor, m
I	Initiator, -
M	Monomer, -
m	Reaction mixture, -
$\dot{m}_x$	Mass flow rate of x-th component, g/s
Nu	Nusselt number, -
P	Reaction pressure, bar
pe	Polyethylene, -
P_{in}	Reactor inlet pressure, Bar
Pr	Prandtl number, -
p_x	Input variable of x component
$P(x)$	Dead polymer with chain length x, -
Q	Heat transfer, J
r_o	Outside radius of tubular reactor area, cm
r_i	Inside radius tubular reactor area, cm
R	Ideal gas constant, cal/(mol·K)
$R(x)$	Live radical with chain length x, -

Re	Reynolds number, -
R_f	Fouling resistance, cm^2·s·K/cal
R_{fmax}	Maximum fouling resistance, cm^2·s·K/cal
S	Solvent, -
ΔT_{ad}	Adiabatic temperature rise, °C
ΔT_{lm}	Log mean temperature, -
T_{in}	Reactor inlet temperature, °C
T_J	Reactor jacket temperature, °C
T_{max}	Maximum reaction temperature, °C
$T_{c,max}$	Maximum reaction critical temperature
T_{cpeak}	Peak critical temperature, °C
U	Overall heat transfer coefficient, cal/(cm^2·s·K)
u_x	Control variable of x component,
v	Linear velocity of the reaction mixture in reactor, cm/s
V_i	Vinyl group
V_{id}	Vinylidene group
V_m	Specific volume of monomer, cm^3/g
V_p	Specific volume of polymer, cm^3/g
$\Delta V_{x,i}$	Activation volume of x component with i-th number, l/mol
X_M	Monomer conversion, %
z	Axial distance from reactor inlet, cm

Greek symbols

λ_x	x-th moment of the live polymer radical, -
μ_x	x-th moment of dead polymer radical, -
β	Beta scission of secondary radical, -
$\beta 1$	Beta scission of tertiary radical, -
$\varnothing$	Diameter
ρ	Reaction mixture density, g/cm^3
η_s	Viscosity of reactant mixture, P
η_r	Relative viscosity of monomer, P
η_o	Viscosity of monomer, P
η_s	Viscosity of reaction,P
w_m	Weight fraction of monomer, -
w_p	Weight fraction of polymer, -

Acknowledgment

REFERENCES

[1] M.K. Chang, J. Ind. Eng. Chem. 27 (2015) 96-101

[2] V.P. Haribal, Y. Chen, L. Neal, F. Li, Eng. J. 4 (2018) 714-721

[3] LDPE EVA Market Outlook, Nexant, Inc., Asia Petrochemical Industry Conference, Japan, 2017, pp. 121-125

[4]   C.H. Chen, J.G Vermeychuk, J.A. Howell, P. Ehrlich, AIChE J. 22 (1976) 463–471

[5]   D. Muhammad, Z. Ahmad, N Aziz, IOP Conf. Ser.: Mater. Sci. Eng. 736 (2020) 042014

[6]   A. Azmi, N. Aziz, International J. Appl. Eng. Res. 11 (2016) 9906-9913

[7]   F.Z Yao, Master Thesis, Nanchang University, 2004

[8]   N. Agrawal, PhD Thesis, National University of Singapore, 2008

[9]   M. Asteasuain, A. Brandolin. Comput. Chem. Eng. 32 (2008) 396-408

[10] A. Azmi, Sudibyo, S.A. Sata, N. Aziz, AIP Conference Proceedings, 2018

[11] F. Stoessel, Thermal Safety of Chemical Processes: Risk Assessment and Process Design, Wiley-VCH, New York, 2008

[12] M. Asteasuain, S. Pereda, M.H. Lacunza, P.E. Ugrin, A. Brandolin. Polym. Eng. Sci. 41 (2001) 711-726

[13] J.S. Tse, Eng. J. 5 (2019) 421-433

[14] A. Azmi, N. Aziz, Procedia Eng. 148 (2016) 1170-1176

[15] C. Kiparissides, A. Baltsas, S. Papadopoulos, J.P. Congalidis, J.R. Richards, M.B. Kelly, Y. Ye, Ind. Eng. Chem. Res. 44 (2005) 2592-2605

[16] D. Kim, P.D. Iedema, Chem. Eng. Sci. 59 (2004) 2039--2052

[17] R.C.M. Zabisky, W.M. Chan, P.E. Gloor, A.E. Hamielec, Polymer 33 (1992) 2243-2262

[18] A. Buchelli, M.L. Call, A.L. Brown, A. Bird, S. Hearn, J. Hannon, Ind. Eng. Chem. Res. 44 (2005) 1474-1479

[19] J.M. Coulson, J.F Richardson, J.R. Backhurst, J.H. Harker, Chemical Engineering: Fluid Flow, Heat Transfer and Mass Transfer, Vol. I, 5th ed., Butterworth-Heinemann, Oxford, 1996

[20] A. Azmi, S. A. Sata, F.S. Rohman, N. Aziz, J. Phys.: Conf. Ser. 1349 (2019) 012094

[21] H. Mavridis, C. Kiparissides, Polym. Proc. Eng. 3 (1985) 263-290

[22] M Cizniar, Diploma Work, Slovak Technical University in Bratislava, 2005

[23] J.E. Cuthrell, L.T. Biegler, AIChE J. 33 (1987) 1257-1270

[24] E.S. Lopez-Saucedo, I.E. Grossmann, J.G. Segovia-Hernandez, S. Hernández, Chem. Eng. Res. Des 111 (2016) 83-99

[25] D. Rodrigues, D. Bonvin, Optim. Control Appl. Methods (2019) 1-20

[26] B.Houska, H. J. Ferreau, M. Diehl, Optim. Control Appl. Methods 32 (2011) 298-312

[27] W. Yan, Y. Qian, W. Ma, B. Zhou, Y. Shen, F. Lin, Eng. J. (2017) 701-707

[28] B. Srinivasan, S. Palanki, D. Bonvin, Comput. Chem. Eng. 27 (2003) 1-26

[29] M. Vallerio, F. Logist, P.V. Erdeghem, C. Dittrich, J.V. Impe, Ind. Eng. Chem. Res. 52 (2013) 1656−1666

[30] H.A. Zogg, "Zurich" Hazard Analysis: A Brief Introduction to the "Zurich" Method of Hazard Analysis Zurich Insurance Group, Risk engineering, 1987.

A. AZMI
S.A. SATA
F.S. ROHMAN
N. AZIZ

School of Chemical Engineering, Engineering Campus, Universiti Sains Malaysia, Seri Ampangan 14300 Nibong Tebal, Seberang Perai Selatan, Penang, Malaysia

NAUČNI RAD

DINAMIČKA OPTIMIZACIJA PROIZVODNJE POLIETILENA NISKE GUSTINE U CEVNOM REAKTORU POD OGRANIČENJEM TERMIČKE SIGURNOSTI

Komercijalni polietilen niske gustine (LDPE), koji se proizvodi postupkom polimerizacije etilena u prisustvu inicijatora u dugačkom cevnom reaktoru, najčešće se koristi u industriji polimera. Veoma egzotermna priroda procesa polimerizacije LDPE i preduslov grejanja i hlađenja u cevnom reaktoru mogu dovesti do različitih problema, posebno sigurnosti u pogledu nekontrolisane promene temperature i produktivnosti, tj. smanjenja konverzije monomera. Zbog toga je potrebno primeniti optimizaciju zasnovanu na modelu industrijskog cevnog reaktora za proizvodnju LDPE uz razmatranje termičke sigurnosti. Prvi osnovni model za ovaj proces je razvijen i potvrđen korišćenjem industrijskih podataka. Bilansi mase i energije izvedeni su iz kinetike polimerizacije LDPE. Nakon toga, razvijen je izraz za temperature u reaktoru pod kritičnim uslovima i uključen u referentni model za proučavanje toplotne sigurnosti. Da bi se osiguralo da je postupak termički bezbedan i da zadovoljava željeni kvalitet proizvoda, pretpostavljena je ograničena dinamička optimizacija, kako bi se maksimalno povećala konverzija monomera, pomoću ortogonalne kolokacije. Rezultati dinamičke optimizacije pokazuju da se maksimalna reakciona temperatura pod kritičnim uslovima može zadovoljiti optimizacijom omotača reaktora. Štaviše, postiže se bez ugrožavanja konverzije monomera i kvaliteta proizvoda.

Ključne reči: Polietilen niske gustine, cevni reaktor, dinamička optimizacija, toplotna sigurnost.